

Effects of pressure on the local atomic structure of CaWO_4 and YLiF_4 : Mechanism of the scheelite-to-wolframite and scheelite-to-fergusonite transitions

D. Errandonea^{1,2}, F.J. Manjón^{3,†}, M. Somayazulu¹, and D. Häusermann¹

¹*HPCAT, Carnegie Institution of Washington, Advanced Photon Source, Building 434E, Argonne National Laboratory, 9700 South Cass Ave., Argonne, IL 60439, U.S.A.*

²*Departamento de Física Aplicada-ICMUV, Universitat de València, Edificio de Investigación, c/Dr. Moliner 50, 46100 Burjassot (Valencia), Spain*

³*Departamento de Física Aplicada, Universitat Politècnica de València, Pl. Ferrandiz i Carbonell 2, 03801 Alcoy (Alicante), Spain*

Abstract: The pressure response of the scheelite phase of CaWO_4 (YLiF_4) and the occurrence of the pressure induced scheelite-to-wolframite (M-fergusonite) transition are reviewed and discussed. It is shown that the change of the axial parameters under compression is related with the different pressure dependence of the W-O (Li-F) and Ca-O (Y-F) interatomic bonds. Phase transition mechanisms for both compounds are proposed. Furthermore, a systematic study of the phase transition in 16 different scheelite ABX_4 compounds indicates that the transition pressure increases as the packing ratio of the anionic BX_4 units around the A cations increases.

PACS.: 61.10.Nz, 61.50.Ks, 62.50.+p

[†] Corresponding author: fjmanjon@fis.upv.es, Tel.(+34) 96 652 84 42, FAX: (+34) 96 652 84 09

1. INTRODUCTION

Many ABX_4 compounds, like calcium tungstate ($CaWO_4$) and yttrium lithium fluoride ($YLiF_4$), crystallize in the tetragonal scheelite structure (SG: $I4_1/a$, No. 88, $Z=4$) [1, 2] at ambient conditions. The strong interest in their structural stability of scheelite compounds under compression is evident by the numerous experimental studies on the pressure effects on their phase behaviour [3 - 14]. In particular, it has been demonstrated recently that $CaWO_4$ transforms under compression from the scheelite structure to the monoclinic wolframite structure (SG: $P2/c$, No. 13, $Z=2$) [1, 2] at 11 ± 1 GPa [3, 4]. On the other hand, $YLiF_4$ transforms under compression from the scheelite structure to the monoclinic M-fergusonite structure (SG: $C2/c$, No. 15, $Z=4$) [1, 2] also at 11 ± 1 GPa [5, 6]. In both compounds, the reversibility to the initial scheelite structure after decreasing pressure has been shown.

From the cationic point of view, the scheelite structure consists of two intercalated diamond lattices: one for A cations and another for B cations (see **Fig. 1**), where the A-A distances are equal to B-B distances. In the scheelite structure A cations, calcium (Ca) and yttrium (Y), are coordinated by eight X anions, oxygen (O) or fluorine (F), thus forming AX_8 polyhedra. On the other hand, B cations, tungsten (W) and lithium (Li), are coordinated by four X anions forming relatively isolated BX_4 tetrahedra [7]. In the cation coordination notation for ABX_4 compounds ([cation A coordination – cation B coordination]) scheelites have cation coordination [8 – 4]. **Fig. 1** shows a detail of the scheelite structure with the AX_8 and BX_4 polyhedra.

The study of the pressure effects on the local atomic structure can be a powerful tool to understand the transformation mechanisms of pressure-driven transitions. While a

systematic analysis of the effects of pressure on the local atomic structure of YLiF₄ has already been performed [5], the same analysis in CaWO₄ has not been performed yet. In this work, we report and discuss the pressure response of the local structure of W (Li) ions in CaWO₄ (YLiF₄) on the light of recently reported high-pressure x-ray diffraction data [3, 5] and other high-pressure techniques. The aim of discussing the effect of pressure in the local structure of both compounds is to understand more precisely the occurrence of the scheelite-to-monoclinic transitions, and particularly, the scheelite-to-wolframite and scheelite-to-fergusonite transitions. From the characterization of the similarities and differences of the pressure response of the local structure of CaWO₄ and YLiF₄ possible transformation mechanisms for both transitions are identified.

2. EXPERIMENTAL BACKGROUND

The lattice parameters and bond distances here presented for CaWO₄ were obtained from energy-dispersive x-ray powder diffraction (EDXD) patterns measured at the X-17C beamline at the National Synchrotron Light Source (NSLS) using a diamond-anvil-cell (DAC) at a diffraction angle $2\theta = 13^\circ$. As CaWO₄ is soft (bulk modulus, $B_0 = 77$ [3]) it was used as its own quasi-hydrostatic pressure medium. A detailed description of these experiments was given in Ref. [3]. There, we reported the occurrence of the scheelite-to-wolframite transition of CaWO₄ at 11 GPa and the amorphization of it at 40 GPa, but we did not discuss the pressure effects on the local structure of the scheelite phase of CaWO₄. In the present paper, we report a detail analysis of this issue by comparing the pressure response of the local structure of CaWO₄ and YLiF₄, in order to better understand the structural pressure behaviour of the scheelite-type ABX₄

compounds. With the aim of illustrating the quality of the structural refinements used to extract the lattice parameters and bond lengths of CaWO_4 here presented, in **Fig. 2** we show an x-ray diffraction pattern of CaWO_4 measured at 2 GPa together with the difference between the measured data and the calculated profile. In order to obtain the lattice parameters from the experimental data the Le Bail extraction technique [15] available in the GSAS programme [16] was employed. For every analyzed pressure we obtained good agreement between the refined profiles and the experimental diffraction patterns, as illustrated in **Fig. 2**, and a low value for the residual for the intensities, $R(F) < 0.15$ (for 52 reflections). The bond distances for CaWO_4 were calculated after performing the structural refinements using the POWDERCELL programme package [17]. For the comparison, the YLiF_4 data were obtained from Grzechnik *et al.* [5] that report data obtained from angle-dispersive powder diffraction experiments performed at the ID9 beamline at the European Synchrotron Radiation Facility using a monochromatic beam ($\lambda = 0.4203 \text{ \AA}$) and a DAC with methanol-ethanol as pressure medium.

3. RESULTS AND DISCUSSION

3.1 Pressure effects on the local atomic structure

In order to know the microscopic mechanisms that govern the scheelite-to-monoclinic phase transitions in CaWO_4 and YLiF_4 we have analyzed the pressure dependence of the lattice parameters and bond distances in these two compounds. **Fig. 3** shows the pressure dependence of lattice parameters for the scheelite phase of CaWO_4 and YLiF_4 . Both compounds show a clearly anisotropic character, the compressibility of the c axis being larger in CaWO_4 , and the compressibility of the a axis being larger in

YLiF₄. This behaviour is reflected in **Fig. 4**, which shows that the c/a ratio in both compounds evolves in a different way under pressure, being c more compressible than a in CaWO₄ while the contrary is true for YLiF₄. The axial ratio c/a decreases under compression from 2.17 at ambient conditions [8] to 2.136 at 11.3 GPa in CaWO₄ [3], but increases from 2.08 at ambient conditions to 2.12 at 11 GPa in YLiF₄ [5]. This different behaviour of the c/a ratio under pressure in CaWO₄ and YLiF₄ was previously noted by the different linear compressibilities of the lattice parameters measured in these compounds [18].

In order to better understand the different anisotropic behaviour of both scheelites under pressure, it is very useful to describe them in terms of the pressure response of the AX₈ and BX₄ polyhedra. With this aim, the pressure dependence of the W-O distances inside the BX₄ tetrahedra and the Ca-O distances inside AX₈ polyhedra are plotted in **Fig. 5** for CaWO₄. The small pressure dependence of the W-O distance, as compared to that of the Li-F distance (see Ref. [5]), indicates that WO₄ tetrahedra are rigid and isolated structural elements that undergo little change with pressure to 11 GPa, unlike LiF₄ tetrahedra, which are more compressible in the same pressure range. On the other hand, Ca-O (Y-F) bond compression is significantly greater (smaller) than that of W-O (Li-F) bonds. These differences in the compressibilities are the cause of the decrease (increase) of the c/a axial ratio in CaWO₄ (YLiF₄).

It is well known that application of pressure reduces the interatomic distances and the atomic sizes, being the large anions more compressible than the small cations [19, 20]. Therefore, the effect of pressure is twofold:

- i) with increasing pressure the decrease of the interatomic distances and of cation sizes leads to an increase of the cation-cation repulsive forces [7, 21]; and
- ii) the reduction of anion sizes leads to an increase of the packing efficiency of anions in the cationic sublattice.

According to Sleight [7], the increase of the cation-cation repulsion forces leads to a decrease of the c/a ratio tending to 2 in tetragonal ABX_4 compounds. This c/a value corresponds to that of the ideal structure for equal near-neighbours cation-cation distances and consequently to equal cation coordination. On the other hand, the increase of the anion packing efficiency leads to an increase of the c/a ratio and consequently to different cation coordination numbers.

Based upon these considerations, we think that the effect of pressure on the phase transitions depends greatly on which of the two above mechanisms predominate with the increase of pressure: cation-cation repulsion, or anion packing efficiency. In this sense, it must be noted that the scheelite structure of $YLiF_4$ at ambient pressure is closer to $c/a = 2$ than that of $CaWO_4$, and with increasing pressure this latter compound tends to the ideal structure for equal cation coordination while the former apparts from it. On this basis, it can be concluded that the high-pressure phase transition of scheelites and the cation coordination of the high-pressure phase could be deduced with the help of the pressure dependence of the c/a ratio. In $CaWO_4$ and $YLiF_4$ cation coordination is [8 – 4]. The decrease of the c/a ratio in $CaWO_4$ with increasing pressure leads to a structure with cation coordination [6 – 6] as it is indeed in the wolframite structure. On the contrary, the increase of the c/a ratio in $YLiF_4$ with increasing pressure leads to a structure with different cation coordination as it occurs in M-fergusonite, with a cation coordination

between $[8 - 4]$ and $[8 - 6]$. It is interesting to note that a similar increase of the c/a ratio with increasing pressure has been recently calculated in the ionic perrhenates AgReO_4 and NaReO_4 [22]. The scheelite perrhenates usually transform at high pressures to the orthorhombic pseudoscheelite structure, whose cation coordination is similar to that of scheelite and M-fergusonite structures.

Experimental results agree with previous considerations because the larger c/a ratio for CaWO_4 than for YLiF_4 indicates that the WO_4 group is more covalent than the LiF_4 group, as it is indeed, and consequently there are smaller cation-cation repulsion forces in CaWO_4 than in YLiF_4 at ambient pressure. However, with increasing pressure cation-cation repulsion forces become dominant in CaWO_4 while packing considerations become dominant in YLiF_4 due to the increase in the covalency of the Y-F and Li-F bonds with increasing pressure. The decrease of the axial ratio in CaWO_4 with increasing pressure, specially above 5 GPa, could be related to just a small increase of the cation-cation electrostatic repulsion, which can be tentatively ascribed to a change in the electronic density around the Ca and W atoms. Furthermore, the change of cation coordination at the scheelite-to-wolframite transition could be originated by a s - d charge transfer effect [3]:

- i) at low-pressure the occupation of the s orbital is favored [23], resulting in a more symmetrical distribution; and
- ii) at high pressures the occupation of a localized d orbital might induce a strong distortion, which would favor the transition to the wolframite structure as it happens in the temperature-driven tetragonal-to-monoclinic transition of BiVO_4 [24].

On the other hand, the increase of the axial ratio in YLiF_4 has been previously ascribed to the big ionic character of the fluorine bonds as compared to those formed by oxygen, the Y-F bond being less ionic and considerably less compressible than the Li-F bond. Therefore, the increase of the tetragonal distortion with increasing pressure was understood due to the big initial compressibility of the Li-F bond. The saturation of the increase of the axial ratio in YLiF_4 above 6 GPa could be related to the stiffening of the Li-F bond leading to a small increase of the cation-cation repulsion at the Li sites with increasing pressure due to the small size of Li atoms.

Another interesting fact is that the reconstructive scheelite-to-wolframite transition in CaWO_4 occurs together with a collapse of both the W-O bonds ($1.798 \text{ \AA} \rightarrow 1.698 \text{ \AA}$) and the Ca-O bonds ($2.293 \text{ \AA} \rightarrow 2.183 \text{ \AA}$ and $2.379 \text{ \AA} \rightarrow 2.272 \text{ \AA}$) at the phase transition. The reduction observed in the Ca-O distance is coherent with the occurrence of a change of the Ca ionic radii from 1.12 \AA (when Ca to O coordination is 8 in the scheelite phase) to 1 \AA (when Ca to O coordination is 6 in the wolframite phase) whereas the reduction of the W-O distances could be related to a change of the character of the bond. On the other hand, the fact that both bonds collapse at the transition is reflected in the fact that the axial ratio remains nearly constant during the transition (the $2c/a$ ratio of the high-pressure wolframite phase is equal to the c/a ratio of the scheelite phase before the transition [3]). In addition, the scheelite-to-wolframite transition produces a distortion of the planes perpendicular to c . Basically, the crystal is deformed along one direction, making $b > a$. This fact is likely related to a tilting of the W – O polyhedra that could easily explain the occurrence of the scheelite-to-wolframite transition.

3.2 Phase transition mechanisms

In order to understand the scheelite-to-wolframite and scheelite-to-fergusonite transitions we have to note that:

- i) the ionic-covalent bonds in the ABX_4 fluorides are much weaker than the more covalent bonds in ABX_4 oxides;
- ii) long bonds are usually softer and more compressible than short ones;
- iii) with increasing pressure almost all bonds become shorter (and most of them stronger); and
- iv) with increasing pressure cation-cation repulsive interaction increases considerably.

On this basis, it is commonly accepted that the atomic structures of ABX_4 compounds under high pressures should tend to structures with a higher and equal coordination of both A and B cations [20]. The structural phase transitions shown by $CaWO_4$ and $YLiF_4$ point towards this direction since both high-pressure monoclinic phases (wolframite and M-fergusonite) show a higher average cation coordination than that of scheelite ([8 - 4]). In the wolframite structure, each A and B cation is in an approximately octahedral coordination surrounded by six near X sites [3, 7]; i.e., with cation coordination [6 - 6], as shown in **Fig. 6(a)**. A view of the cations in the wolframite structure is shown in **Fig. 6(b)**. The [6 - 6] coordination in the wolframite phase suggests similar strengths for the forces associated to the W-O and Ca-O bonds in such structure and points to an increase of the coordination number around W cations with increasing pressure in the scheelite phase of $CaWO_4$. On the other hand, in the M-fergusonite structure, each A cation is surrounded by eight X anions and each B cation is surrounded by four X sites and two additional near X sites. Therefore, the M-fergusonite structure is considered as a deformed scheelite structure, which can be described as an intermediate

structure between [8 - 4] and [8 - 6] cation coordination. **Fig. 7** shows two views of the cation arrangement in the M-fergusonite structure.

The mechanism of the scheelite-to-wolframite transition in CaWO_4 around 11 GPa is of reconstructive nature and involves the destruction of both the diamond-like structures of Ca and W cations of the scheelite structure at the transition pressure. This reconstructive transition is due to the similar cation-cation repulsion forces at the Ca and W sites at the transition pressure that corresponds to similar Ca-O and W-O forces at the phase transition pressure. It is noteworthy the similarity of Ca-O and W-O forces at the transition pressure despite the ionic and the covalent characters of the Ca-O and W-O bonds at ambient pressure, respectively [25]. From a short-range point of view, this phase transition mechanism is related to a shift of the W cation from the center of the WO_4 tetrahedron towards the center of the WO_6 octahedron, and it is characterized by:

- i) a motion of the W atoms from the center of the W-O tetrahedra along the b direction; and
- ii) a shear displacement of its second neighbours O atoms.

Fig. 8(a) shows a schematic representation of the scheelite-to-wolframite transformation mechanism and **Fig 8(b)** shows the (100) projection of a section of the scheelite structure compared with that of a portion of the wolframite structure in order to illustrate better the transformation. We believe that the process leading to the scheelite-to-wolframite transition is the following: At low pressure, the weak Ca-O bonding of the CaO_8 polyhedra absorb much of the pressure while the WO_4 tetrahedra remain as rigid units. Around 10 GPa, the Ca-O bond length decreases more than the W-O bond length so as to become as strong as the W-O bond (see **Fig. 5**). Upon further application of

pressure, the W-O tetrahedral units are tilt and distorted and the [010] planes shear forming a distorted “star of david” (see **Fig. 8(b)**). This configuration is characteristic of a cation in octahedral coordination when viewed perpendicular to the *c* axis of the scheelite (with four O atoms at 1.698 Å from W and two O atoms at 1.898 Å from W in the distorted octahedron).

On the other hand, the mechanism of the scheelite-to-M-fergusonite transition in YLiF₄ around 11 GPa is of martensitic nature and it is preceded by a reversible polytype phase transition at 6 GPa. The LiF₄ tetrahedra in the scheelite structure of YLiF₄ form an angle $\phi = 29^\circ$ with respect to the main *a* axis at ambient pressure [18]. With increasing pressure, the Li-F distance decreases till the LiF₄ tetrahedra become rigid around 6 GPa. At higher pressures, the stiffening of the Li-F bond and the progressive decrease of the *a* lattice parameter above 6 GPa (see **Fig. 4** in **Ref. 5**) is only possible if there is a gradual rotation of the LiF₄ tetrahedra around the tetragonal *c* axis; i.e. in the *a-b* plane, towards larger angles. This means that the LiF₄ tetrahedra can only rotate till the maximum value of $\phi = 45^\circ$ compatible with the scheelite structure and the reduction of the *a* lattice parameter. This rotation can be considered as a reversible phase transition from a polytype-I to a polytype-II scheelite structure. The polytype I is characterized by a setting angle $\phi = 29^\circ$, closer to the higher symmetry zircon structure with $\phi = 0^\circ$, while the polytype II is characterized by an angle ϕ ($29^\circ < \phi < 45^\circ$). The reversible phase transition from scheelite polytype-I to polytype-II is induced by polyhedral tilting (in this case rotation in the *a-b* plane). This phase transition is possible due to the softening of one of the translational T(E_g) modes of the scheelite phase that involves a rotation of the LiF₄ tetrahedra in the plane perpendicular to the *c* axis [28]. It is worth noting that the

softening of the $T(E_g)$ mode of the zircon phase of YVO_4 is also the responsible for the zircon-to-scheelite phase transition above 7.5 GPa [29], since the VO_4 tetrahedra in the zircon phase form an angle $\phi = 0^\circ$ with respect to the main a axis while that angle is always different from $\phi = 0^\circ$ in the scheelite structure.

A characteristic of this kind of reversible transitions is that the low-pressure structure (with higher symmetry) shows a certain degeneration of the vibrational modes that disappear once the phase transition to the low-symmetry structure is accomplished [27]. A splitting of several Raman modes above 6 GPa that were initially overlapped is indeed observed [12,13]. Furthermore, this structural change around 6 GPa in $YLiF_4$ is reflected in a slight modification of the frequency pressure coefficients of some Nd^{3+} crystal-field transitions above 6 GPa [6].

Reversible transitions show no major change in cation coordination, except for subtle displacements in the cation coordination of those cations with larger coordination number, and occur in a sudden and reversible way leaving the crystal lattice undamaged during the transformation and with reduced volume changes. Furthermore, the reversible transitions are usually followed by twinning; i.e., a mixture of different lattice orientations of the new crystals due to the loss of a symmetry element in the phase transition. This effect can affect the accurate determination of the lattice parameters in the new structure and could be related to the strange behaviour of the distances estimated in **Ref. 5** from high-pressure X-ray diffraction measurements between 6 and 11 GPa. Furthermore, the reversible phase transition around 6 GPa is coherent with the martensitic phase transition occurring at 10 GPa in $YLiF_4$ since both reversible and martensitic transitions are common in ionic compounds [30, 31] and have been also

found in other similar compounds like KAlF_4 and RbAlF_4 as a function of temperature and pressure [32, 33].

Finally, the martensitic scheelite-to-M-fergusonite transition is a shear transformation in which the initial structure is partially conserved while certain sheets or pieces of the previous structure are slightly shifted. In YLiF_4 , it involves a shift of long zig-zag chains of B (Li) cations either along [100] or along [010] directions of the scheelite structure (see the schematic model shown in **Fig. 9**). Previous studies suggest that layer shifts along the [100] direction are energetically more favorable than shifts along [010] direction [26]. The large shift of the B cations in YLiF_4 in contrast to CaWO_4 is due to the mainly ionic character of the Li-F bond that is much weaker than the covalent W-O in CaWO_4 ; making Li less tightly bound than W in the scheelite structure. This type of transitions is quick and in certain cases the crystal is undamaged despite the symmetry of the final structure is lower than that of the previous one. These transformations are usually reversible; i.e., the initial structure is recovered on release of pressure, but they use to show a certain hysteresis; a behavior indeed found in the scheelite-to-M-fergusonite phase transition in YLiF_4 above 10 GPa [6].

This phase transition takes place because cation-cation repulsion increases considerably above 10 GPa, especially at the Li sites, what leads to the destruction of the Li diamond-like structure at the transition pressure whereas the Y diamond-like structure is preserved and slightly distorted. This well-known high-pressure structure is related to the scheelite structure, since it can be considered as a distorted scheelite (see the comparison view of both structures in **Fig. 9**), and conversely the scheelite structure can be viewed as a tetragonal fergusonite [31]. The larger increase of the repulsion at the Li

sites as compared to the Y sites is likely due to the change in the electronic density around the Y atoms, unlike Li atoms, with increasing pressure because of the *s-d* charge transfer previously commented [34]. The slight distortion of the Y diamond-like lattice and the shift of Li cations allow us to understand the martensitic second-order phase transition nature of the scheelite-to-M-fergusonite transition that proceeds without volume change, as demonstrated by Gingerich and Bair [35].

Several additional facts support the described mechanisms for the above phase transitions in CaWO_4 and YLiF_4 . There is a vision that the oxide scheelites can be considered as having a complex layer-like structure, the layers being perpendicular to the *c* axis and formed by a CsCl-type arrangement of A and BO_4 ions [26]. This view of oxide scheelites as complex layer structures is supported by the large values of the *c/a* ratios of these compounds at ambient conditions, as compared to those of nearly ideal fluoride scheelites. Therefore, the decrease of the axial ratio in CaWO_4 with increasing pressure tending to the ideal structure is in agreement with the tendency of several scheelite oxides to transform to the wolframite structure with increasing pressure [36]. In summary, oxide scheelites show a tendency towards a layer-like structure, unlike fluoride scheelites. In this sense, the high-pressure scheelite-to-wolframite transition is expected in CaWO_4 because the wolframite structure has also a layer-like structure, unlike the M-fergusonite one. The layer-like structure of the wolframite structure along the *a* direction can be observed in **Fig. 6(b)**.

The different tendency of the oxides and fluorides scheelites towards layer-like structure due to their different nature is also reflected in the thermal expansion coefficients of oxide and fluoride scheelites. In fluoride scheelites, the α_{11} tensor

component of the thermal expansion is greater than the α_{33} , whereas in oxide scheelites the contrary is true, as it is usual in layer-like crystals [11, 37]. Furthermore, we believe that the different high-pressure structures observed in both compounds are related to the different nature of bonds in CaWO_4 and YLiF_4 and exhibit a link with the different behavior of the axial compressibilities and the different soft modes observed in both compounds. In this respect, Blanchfield *et al.* noted the instability of these two compounds under application of shear stresses, as deduced from the softening of several lateral modes [10, 11]. However, the soft modes with bigger softening are not the same in CaWO_4 and YLiF_4 , pointing out a significant difference between the two compounds. This result agrees with recent results of ion rigid calculations in YLiF_4 [38] and with recent Raman scattering measurements under pressure [9, 12, 13]. In CaWO_4 a softening of one of the translational zone center $T(B_g)$ modes as pressure increases has been observed [9], while in YLiF_4 the mode that softens under pressure is one of the translational zone center $T(E_g)$ modes [13, 38]. These two modes are interrelated because both can be considered as external modes of the BX_4 tetrahedra and their frequencies are greatly affected by the substitution of the A cation [39]. These vibrational modes are low-frequency modes in both compounds and are associated to translations of the BX_4 tetrahedra. The B_g mode is associated to the vibration of the BX_4 tetrahedra along the tetragonal axis of the scheelite, whereas the E_g mode is related to the vibration of the BX_4 tetrahedra in the plane perpendicular to the tetragonal axis of the scheelite. We think that the softening of these modes is indicative of the increase of the B-B distances observed in the scheelite-to-monoclinic phase transitions.

As a summary, we may conclude that the mechanisms that lead to the scheelite-to-wolframite transition are:

- i) an increase of the B-B distance, due to the traslation of the BX_4 tetrahedra along the c axis but maintaining the same mass center as in the scheelite structure; and
- ii) a tilt of the BX_4 tetrahedra respect to the c axis (see **Fig. 9**). Both the increase of the B-B distance along the c axis of the scheelite and the tilt of the BX_4 tetrahedra can be associated to the softening of the B_g mode.

Correspondingly, the mechanisms that lead to the scheelite-to-M-fergusonite transition are:

- i) a rotation of the BX_4 tetrahedra around the c axis of the scheelite;
- ii) a slight distortion of the Y diamond-like structure; and
- iii) a translation of the BX_4 tetrahedra along the a (or b) directions of the scheelite, leading to an increase of the B-B distance along the $b+c$ (or $a+c$) direction of the scheelite (see **Figs. 1 and 9**). Both the rotation and the traslation along the a or b direction can be associated to the softening of the E_g mode.

3.3 Size Criterion

We have attempted to correlate the packing ratio of the anionic BX_4 units around the A cations and the known phase transition pressures in the scheelite compounds. **Table I** summarises the available data on pressure studies of sixteen different scheelite ABX_4 compounds. In Fig. 10 we have plotted the transition pressure vs. the BX_4/A radii ratio because this ratio is the sum of the X/A plus the B/A effective ionic ratios. As a result, we have observed that phase transition pressure increases as the ratio between the ionic radii

(BX_4/A) increases. From these data it can be obtained the following relation for the transition pressure (P_C):

$$P_C = (1 \pm 2) \text{ GPa} + (10.5 \pm 2) (BX_4/A - 1) \quad . \quad (1)$$

This relationship indicates that for $BX_4/A < 1$ the scheelite structure is not stable even at ambient pressure. To calculate BX_4/A values given in **Table I** the ionic radii of A, B, and X atoms were taken from the literature [51 - 54]. As already commented, both effective ionic radii decrease in cations and anions with increasing pressure with a bigger decrease of the larger anionic radii [19,20]. Therefore, with increasing pressure the B/A ratio is almost constant, while the X/A ratio decreases considerably with increasing pressure. Consequently, it is expected that the BX_4/A ratio decreases with increasing pressure and that those compounds showing a smaller BX_4/A ratio exhibit lower transition pressures as is already empirically found in scheelite compounds.

The above hypothesis for the instability of the scheelite compounds with BX_4/A ratios near or below 1 is supported by the transition pressures found in the alkaline-earth perrhenates and periodates families [40-42, 55]. It has been shown that $KReO_4$, $RbReO_4$, KIO_4 and $RbIO_4$ crystallize in the scheelite structure. However, $TlReO_4$, $CsReO_4$, and $CsIO_4$, showing smaller BX_4/A ratios near 1, crystallize in a pseudoscheelite structure at ambient pressure, being this structure one of the high-pressure phases of perrhenates and periodates crystallizing in the scheelite structure at ambient pressure.

The above given observations suggest that the proposed size criterion (which effectively also applies to A_2BX_4 compounds [56]) could constitute a significant step towards unraveling the mechanisms underlying pressure-driven transformations in scheelite compounds. Particularly, this simple criterion could be useful to predict the

occurrence of pressure-driven instabilities in additional scheelite compounds like, e.g. ZrGeO_4 , NaReO_4 , and NaRuO_4 , for which **Eq. (1)** predicts the occurrence of pressure-driven phase transitions at 14.8 GPa, 11.5 GPa and 7.3 GPa, respectively. It could be also helpful to estimate pressure-driven instabilities even in metastable scheelite compounds at ambient pressure after a pressure cycle, as YVO_4 [57], for which a phase transition near 11 GPa is estimated.

As regards further high-pressure phase transitions in CaWO_4 and YLiF_4 , the wolframite structure of CaWO_4 leads to an amorphous phase above 40 GPa [3]. However, the M-fergusonite structure of YLiF_4 seems to lead to a new high-pressure phase still not determined above 17 GPa [5, 13]. Several reports indicate that M- to M'-fergusonite phase transitions are common in ferroelastic materials under decrease of temperature or increase in pressure [58, 59], the M' phase being isostructural to the baddeleyite structure (SG: $P2_1/c$, No. 14, $Z=2$) [1, 2] or to the wolframite structure [59 - 61]. The M- to M'-fergusonite phase transition is of reconstructive-type with the unit cell of the baddeleyite structure similar to the wolframite unit cell. In this sense, the b axis of the M-fergusonite is almost twice that of the wolframite or the baddeleyite being the a and c axis of the M-fergusonite slightly smaller than those of the wolframite and the baddeleyite. Therefore, a phase transition likely to a baddeleyite (or wolframite) structure is expected for YLiF_4 above 17 GPa. The transition to the baddeleyite structure would be consistent with the baddeleyite structure shown by MnLiF_4 at ambient pressure, being the Mn^{3+} ionic radius smaller than that of Y^{3+} . Thus, the decrease of the Y ionic radius with increasing pressure could increase the instability of the M-fergusonite structure leading to the baddeleyite structure. On the other hand, the transition to the wolframite structure

would be also possible and it has recently been predicted by electronic structure *ab initio* calculations performed using the VASP code [62]. New high-pressure x-ray diffraction studies of YLiF₄ are required to answer definitively the new high-pressure structure.

4. CONCLUDING REMARKS

We report the pressure dependence of the lattice parameters and bond distances of the scheelite phase of CaWO₄ and compare them to those reported for YLiF₄. The comparison of the thermal expansion coefficients and the pressure coefficients found for the lattice parameters, bond distances, and Raman modes in the two compounds has allowed us to understand why these two scheelites do not show the same high-pressure phase transitions. A mechanism for each of the two scheelite-to-monoclinic (wolframite or M-fergusonite) phase transitions has been proposed. Furthermore, from a comparative analysis of sixteen different scheelite compounds a close relationship between the phase transition pressures in scheelites and the BX₄/A ratio has been found. This simple criterion can be applicable to the search of new pressure-induced transformations in scheelite compounds.

Acknowledgements

The authors gratefully acknowledge the contribution of A. Vegas and A. Segura, who reviewed this paper making valuable comments. We also thanks Dr. J. Hu of beam line X-17C at NSLS for valuable technical advice and assistance. This work was supported by the NSF, the DOE, and the W. M. Keck Foundation. Daniel Errandonea

also acknowledges the financial support from the MCYT of Spain through the “Ramon y Cajal” program for young scientists.

References

- [1] R.W.G. Wyckoff, *Crystal Structures*, 2nd ed. (Wiley, New York, 1964), vol. 3, pp 1-67.
- [2] International Tables for Crystallography, vol. A, ed. by T. Hahn (D. Riedel, Boston, 1987).
- [3] D. Errandonea, M. Somayazulu, and D. Häusermann, *phys. stat. sol. (b)* **235**, 162 (2003).
- [4] D. Christofilos, S. Ves, and G. A. Kourouklis, *phys. stat. sol. (b)* **198**, 539 (1996).
- [5] A. Grzechnik, K. Syassen, I. Loa, M. Hanfland, and J. Y. Gesland, *Phys. Rev. B* **65**, 104102 (2002).
- [6] F. J. Manjón, S. Jandl, K. Syassen, and J. Y. Gesland, *Phys. Rev. B* **64**, 235108 (2002).
- [7] A. W. Sleight, *Acta Cryst. B* **28**, 2899 (1972).
- [8] R. M. Hazen, L. W. Finger, and J. W. E. Mariathasan, *J. Phys. Chem. Solids* **46**, 253 (1985).
- [9] D. Christofilos, G. A. Kourouklis, and S. Ves, *J. Phys. Chem. Solids* **56**, 1125 (1995).
- [10] P. Blanchfield, G.A. Saunders, and T. Hailing, *J. Phys. C: Solid State* **15**, 2081(1982).
- [11] P. Blanchfield, T. Hailing, A. J. Miller, G.A. Saunders, and B. Chapman, *J. Phys. C: Solid State* **20**, 3851(1983).
- [12] E. Sarantopoulou, Y. S. Raptis, E. Zouboulis, and C. Raptis, *Phys. Rev.* **59**, 4154 (1999).
- [13] Q. A. Wang, A. Bulou, and J. Y. Gesland, *cond-mat/0210491* (2002).
- [14] D. Errandonea, M. Somayazulu, and D. Häusermann, *phys. stat. sol. (b)* **231**, R1 (2002).
- [15] A. LeBail, H. Duroy, and J. L. Fourquet, *Mater. Res. Bull.* **23**, 447 (1988).
- [16] A. C. Larson and R. B. Von Dreele, *Los Alamos Natl. Lab. Rep. LAUR*, **86** -748 (2000).
- [17] W. Kraus and G. Nolze, *J. Appl. Crystallogr.* **29**, 301 (1996).
- [18] P. Blanchfield, and G.A. Saunders, *J. Phys. C: Solid State* **12**, 4673 (1979).
- [19] O. Fukunaga and S. Yamaoka, *Phys. Chem. Minerals* **5**, 167 (1979).
- [20] J.P. Bastide, *J. Solid State Chemistry* **71**, 115 (1987) and references therein.
- [21] J.W. Otto, J.K. Vassiliou, R. F. Porter, and A. L Ruoff, *Phys. Rev. B* **44**, 9223 (1991).
- [22] J. Spitaler, C. Ambrosch-Draxel, E. Nachbaur, F. Belaj, H. Gomm, and F. Netzer, *Phys. Rev. B* **67**, 115127 (2003).

- [23] Y. Zhang, N.A. Holzwarth, and R.T. Williams, Phys. Rev. B **57**, 12738 (1998).
- [24] L.E. Depero and L. Sangaletti, J. Solid State Chemistry **129**, 82 (1997).
- [25] J. R. Smyth, S. D. Jacobsen and R. M. Hazen, Reviews in Mineralogy **41**, 157 (2000) and references therein.
- [26] A. Arbel and R.J. Stokes, J. Appl. Phys. **36**, 1460 (1965).
- [27] R.G. J. Strens, Mineral Mag. **36**, 565 (1967).
- [28] S.P.S. Porto and J.F. Scott, Phys. Rev. **157**, 716 (1967).
- [29] A. Jayaraman, G. A. Kourouklis, G. P. Epinosa, A. S. Cooper, and L. G. Van Uitert, J. Phys. Chem. Solids **48**, 755 (1987).
- [30] R.M. Hazen and L.W. Finger, *Comparative Crystal Chemistry* (John Wiley, New York, 1982).
- [31] O. Müller and R. Roy, *The major ternary structural families* (Springer, Berlin, 1974).
- [32] A. Bulou, A. Gibaud, M. Debieche, J. Nouet, B. Hennion, and D. Petitgrand, Phase Transitions **14**, 47 (1989).
- [33] Q. A. Wang, G. Ripault, and A. Bulou, Phase Transitions **53**, 1 (1995).
- [34] Y.K. Vohra, H. Olijnik, W. Grosshans, and W.B. Holzapfel, Phys. Rev. Lett. **47**, 1065 (1981).
- [35] K.A. Gingerich and H.E. Bair, Advanc. X-ray Analysis **7**, 22 (1964).
- [36] J. Macavei and H. Schulz, Z. Kristallogr. **207**, 193 (1993).
- [37] V.T. Deshpande, S.V. Suryanarayana, and R.R. Pawar, Act. Crystallogr. A **24**, 398 (1968); V.T. Deshpande and S.V. Suryanarayana, J. Phys. Chem. Solids **30**, 2484 (1969).
- [38] A. Sen, S.L. Chaplot, and R. Mittal, J. Phys.: Condens. Matter **14**, 975 (2002).
- [39] S. Salaün, M. T. Fornoni, A. Bulou, M. Rousseau, P.Simon, and J. Y. Gesland, J. Phys.: Condens. Matter **9**, 6941 (1997).
- [40] T. A. Al Dhahir, H. L. Bhat, P. S. Narayanan, and A. Jayaraman, J. Raman Spectrosc. **22**, 567 (1991).
- [41] N. Chandrabhas and A. K. Sood, Phys. Rev. B **51**, 8795 (1995).

- [42] A. Jayaraman, G.A. Kourouklis, L.G. Van Uitert, W.H. Grodkiewicz and R.G. Maines Sr., Physica A **156**, 325 (1988).
- [43] A. Jayaraman, B. Batlogg, and L. G. Van Uitert, Phys. Rev. B **28**, 4774 (1983).
- [44] D. Christofilos, K. Papagelis, S. Ves, G.A. Kourouklis, and C. Raptis, J.Phys.: Condens. Matter **14**, 12641 (2002).
- [45] D. Errandonea [unpublished].
- [46] A. Jayaraman, B. Batlogg, and L. G. Van Uitert, Phys. Rev. B **31**, 5423 (1985).
- [47] S. R. Shieh, L. C. Ming, and A. Jayaraman, J. Phys. Chem. Solids **57**, 205 (1996).
- [48] A. Jayaraman, S. Y. Wang, S. R. Shieh, S. K. Sharma, and L. C. Ming, J. Raman Spectrosc. **26**, 451 (1995).
- [49] N. Ganguly and M. Nicol, phys. stat. sol. (b) **79**, 617 (1977).
- [50] Q. A. Wang, S. Salaün, and A. Bulou, cond-mat/0210553 (2002).
- [51] R.D. Shannon, Acta Cryst. A **32**, 751 (1976).
- [52] R.D. Shannon and C.T. Prewitt, Acta Cryst. B **25**, 925 (1969).
- [53] R.D. Shannon and C.T. Prewitt, Acta Cryst. B **26**, 1046 (1970).
- [54] J.E. Huheey, E.A. Keiter, and R.L. Keiter, *Inorganic Chemistry: Principles of Structure and Reactivity*, 4th ed. (HarperCollins, New York, 1993).
- [55] N. Chandrabhas, D.V.S. Muthu, A.K. Sood, H.L. Bhat, and A. Jayaraman, J. Phys. Chem. Solids **92**, 959 (1992).
- [56] G. Serghiou, H.J. Reichmann, and R. Boehler, Phys. Rev. B **55**, 14765 (1997).
- [57] G. Chen, N.A. Stump, R.G. Haire, J.R. Peterson, and M.M. Abraham, Solid State Commun. **84**, 313 (1992).
- [58] G.A. Wolten and A.B. Chase, Am. Miner. **52**, 1536 (1967).
- [59] Yu.A. Titov, A.M. Sych, A.N. Sokolov, A.A. Kapshuk, V.Ya. Markiv, and N.M. Belyavina, J. Alloys and Compounds **311**, 252 (2000).

- [60] V.Ya. Markiv, N.M. Belyavina, M.V. Markiv, Yu.A. Titov, A.M. Sych, A.N. Sokolov, A.A. Kapshuk, and M.S. Slobodyanyk, *J. Alloys and Compounds* **346**, 263 (2002).
- [61] G. A. Wolten, *Acta Cryst.* **23**, 939 (1967).
- [62] S. Li, R. Ahuja, and B. Johansson, [to be published].

Table I. *Phase transition pressures and BX_4/A ratios for some scheelite compounds.*

<i>Compound</i>	<i>BX_4/A ratio</i>	<i>P_C (GPa)</i>	<i>Reference</i>
KIO ₄	1.39	6.5	40
RbIO ₄	1.25	5.3	41
AgReO ₄	1.9	13 ± 1	21
KReO ₄	1.45	7.5	42
RbReO ₄	1.30	1.6	42
CaWO ₄	1.89	11 ± 1	3, 4
SrWO ₄	1.76	10.5 ± 2	2, 43, 44
EuWO ₄	1.76	8 ± 1	45
PbWO ₄	1.66	4.5	46
BaWO ₄	1.47	6.5 ± 0.3	43
CdMoO ₄	2.03	12	47
CaMoO ₄	1.88	8.2 ± 0.4	9
SrMoO ₄	1.74	12.5 ± 0.5	48
PbMoO ₄	1.64	6.5 ± 3	46, 49
CaZnF ₄	1.97	10	50
YLiF ₄	2.11	11 ± 1	5, 6, 13

Figure captions

Figure 1. Unit cell of the scheelite structure of ABX_4 compounds with the a , b and c axis. Big atoms refer to A cation (Ca, Y), medium-size atoms correspond to B cations (W, Li) and small atoms to the X anion (O, F). Numbers 1 and 2 correspond to B-B distances of the diamond-like structure along $b + c$ and $a + c$ directions, respectively. The AX_8 polyhedra and the BX_4 tetrahedra are shown.

Figure 2: EDXD pattern of the scheelite phase of $CaWO_4$ at 2 GPa. The background was subtracted. The stars mark the position of the diffraction lines of the Au pressure marker. The last line represents the difference between the measured data and the refined profile. The bars indicate the calculated positions of the $CaWO_4$ reflections.

Figure 3. Pressure dependence of the unit cell parameters of the scheelite structure in $CaWO_4$ and $YLiF_4$. Data for $YLiF_4$ (\circ) are taken from Ref. 5 and data for $CaWO_4$ are from the present study (\bullet) and Ref. 8 (\blacksquare).

Figure 4. Pressure dependence of the c/a ratio of the scheelite structure in $CaWO_4$ and $YLiF_4$. Data for $YLiF_4$ (\circ) are taken from Ref. 5 and Data for $CaWO_4$ are from the present study (\bullet), Ref. 7 (\blacklozenge), and Ref 8 (\blacksquare). Lines are just guide for the eye.

Figure 5. Pressure dependence of the interatomic bonds in the scheelite structure of $CaWO_4$. The solid lines show the pressure dependence of the Ca-O bonds and the dashed lines the pressure dependence of the W-O bonds. Solid symbols are from the present study and empty symbols from Ref. 8.

Figure 6. (a) Wolframite structure of $CaWO_4$ with its unit cell and the a , b and c axis. (b) Wolframite structure of $CaWO_4$ in the a - b plane. Big black atoms refer to A cation (Ca),

grey medium-size atoms correspond to B cation (W) and small atoms to the X anion (O). The AX_6 octahedra, the BX_6 octahedra, and the shorter zig-zag cation-cation distances are also shown in (a) while anion atoms are not shown for the sake of clarity in (b). The shorter metal-metal distances are also shown in both schemes.

Figure 7. Schematic views of the cationic arrangement in the M-fergusonite structure. Black atoms correspond to the A cation (Y), grey atoms correspond to the B cation (Li). Anion atoms (F) are not shown for the sake of clarity. The shorter metal-metal distances are also shown.

Figure 8. (a) Schematic representation of the scheelite-to-wolframite model transition mechanism. (b) The (100) projection of a section of the scheelite structure compared to that of a portion of the wolframite structure. 1, 2, and 3 represent oxygens at $(1/4,0,0)$ and 4, 5, and 6 oxygens at $(-1/4,0,0)$.

Figure 9. Detail of the scheelite structure (left) in the a - c plane with A (Y) and B (Li) cations located in alternated planes along the b axis (perpendicular to the paper). Detail of the M-fergusonite structure (right) in the c - b plane with A and B cations located in alternated planes along a axis (perpendicular to the paper). The M-fergusonite structure derives from the scheelite structure when B cations shift along a axis of the scheelite.

Figure 10. Phase transition pressure in several scheelites as a function of the BX_4/A ratio. Symbols correspond to the data summarized in **Table I**, the solid line corresponds to the relation given in **Eq. (1)**, and the dashed lines are its lower and higher deviations.

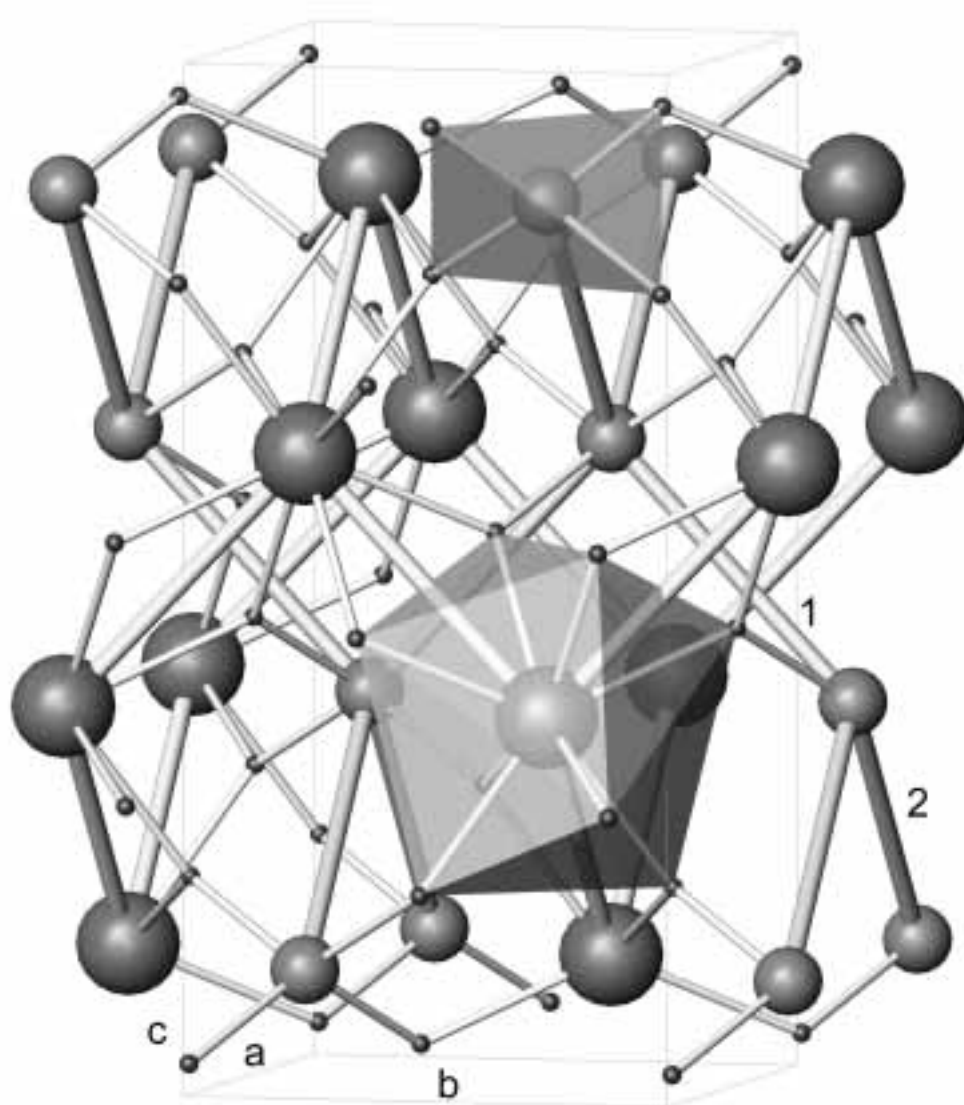


Figure 1. D. Errandonea et al.

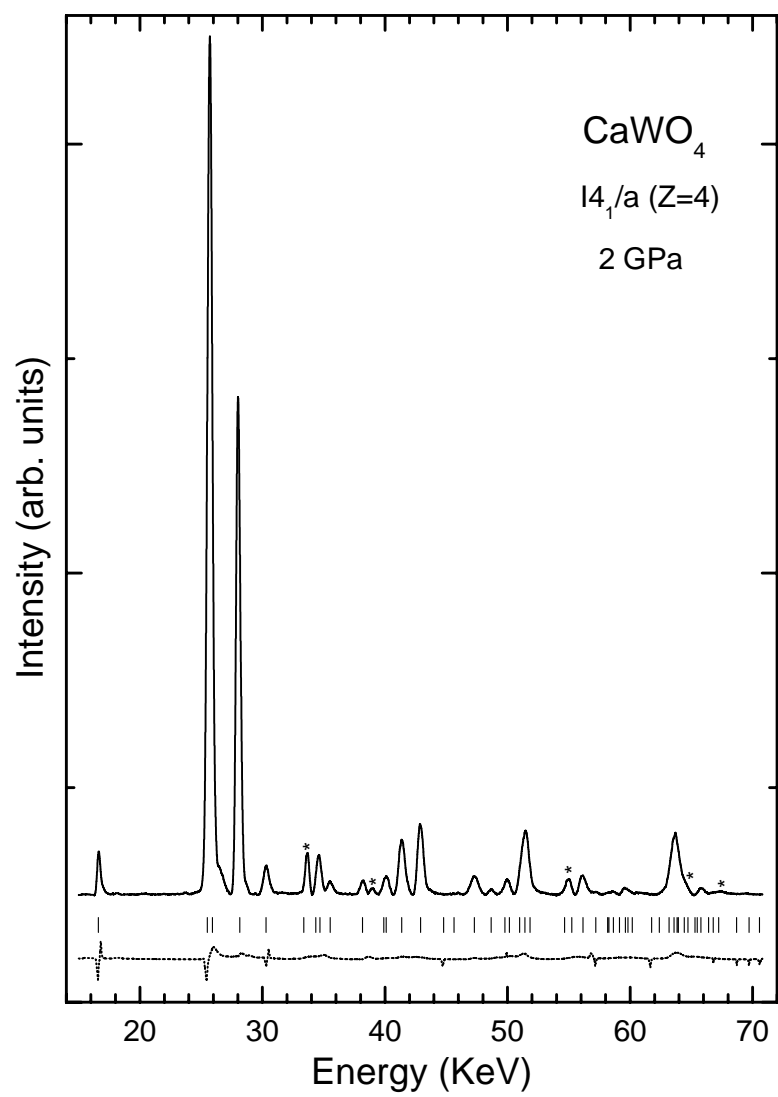


Figure 2. D. Errandonea et al.

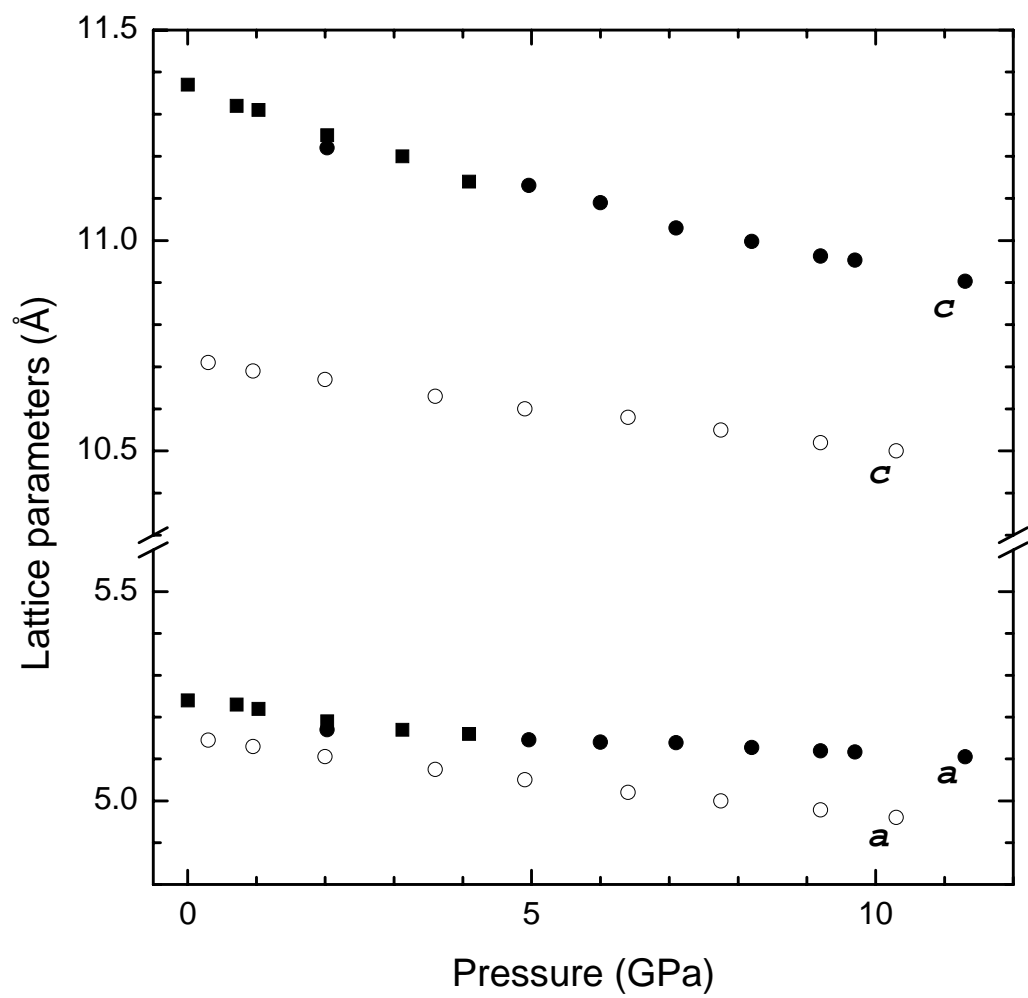


Figure 3. D. Errandonea et al.

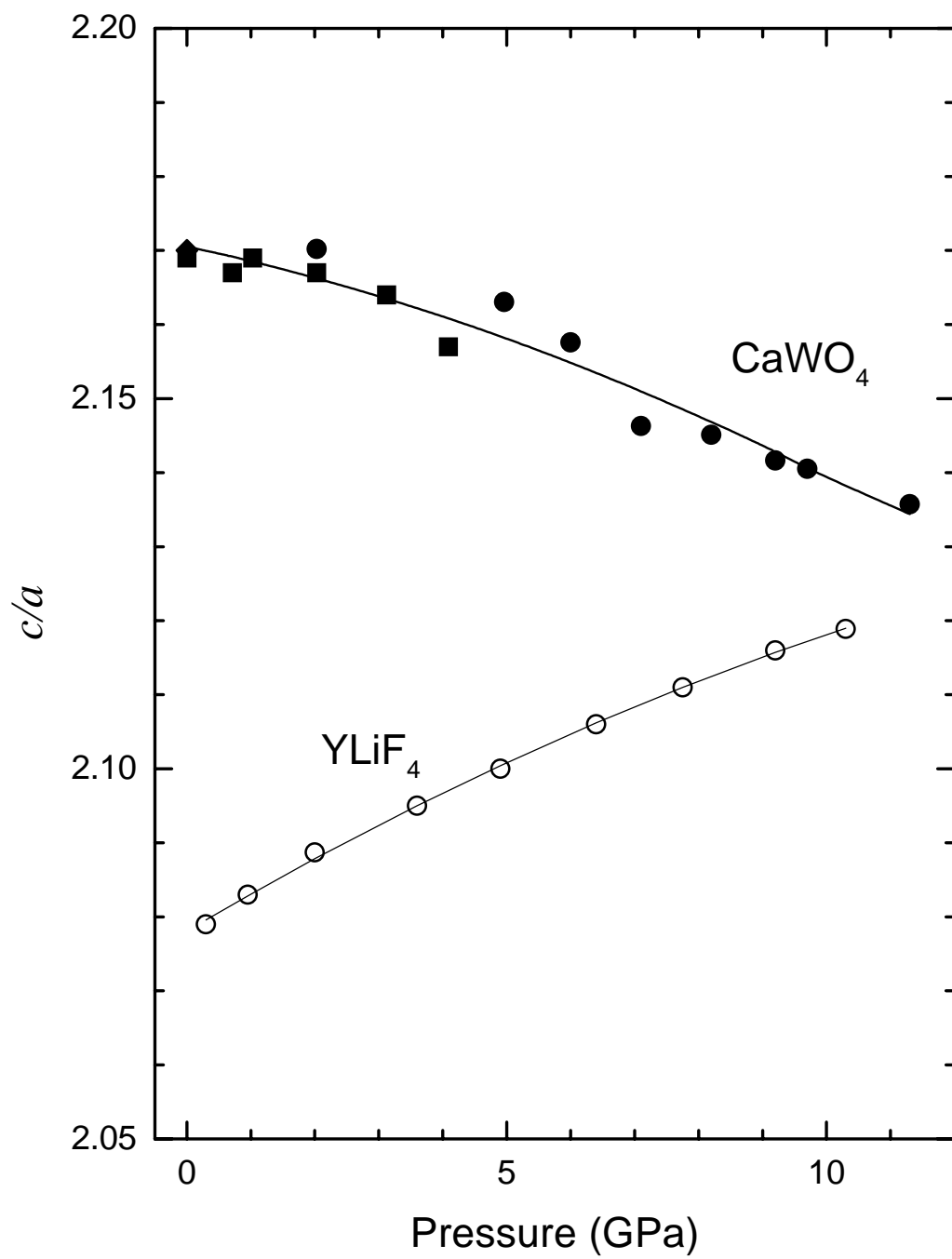


Figure 4. D. Errandonea et al.

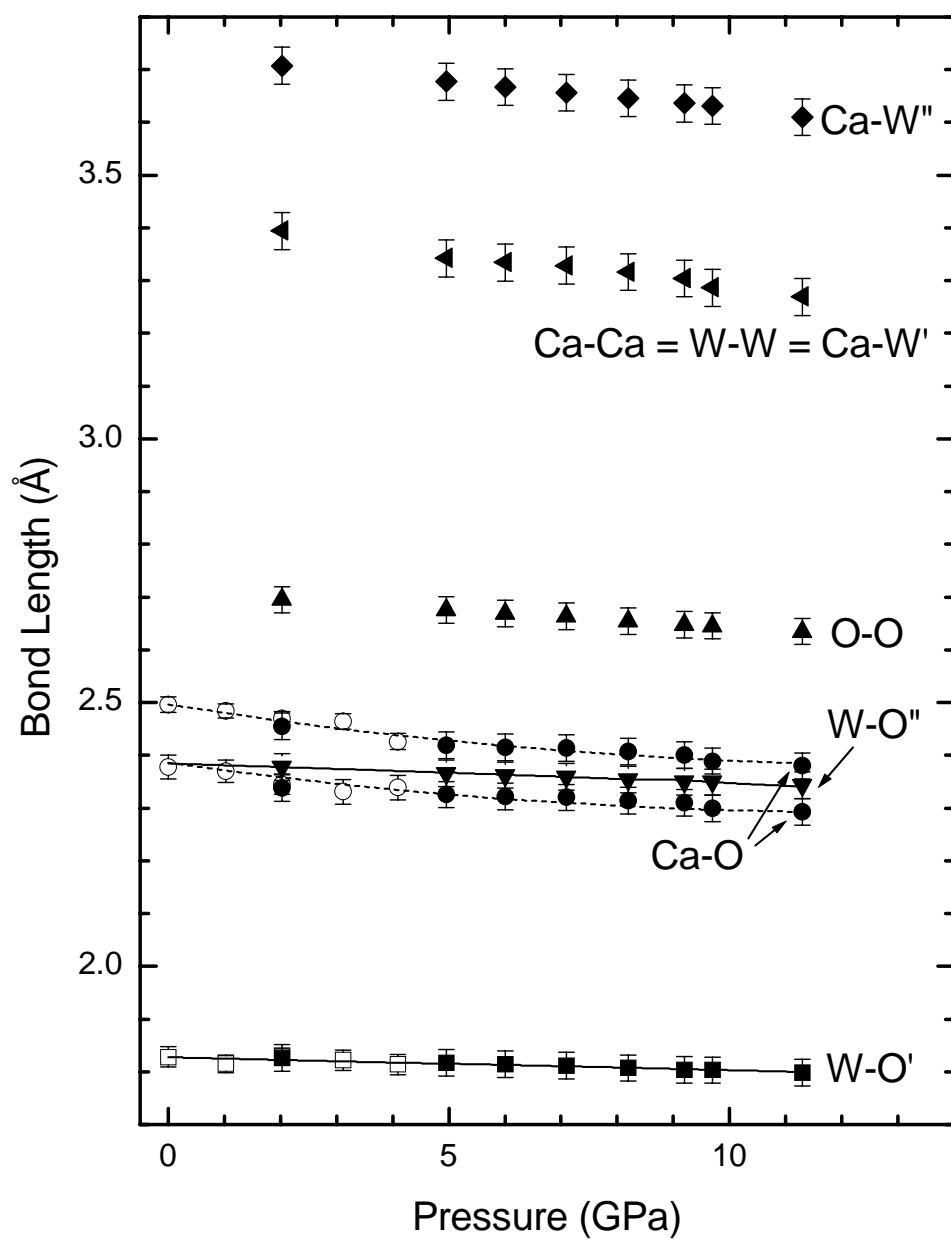


Figure 5. D. Errandonea et al.

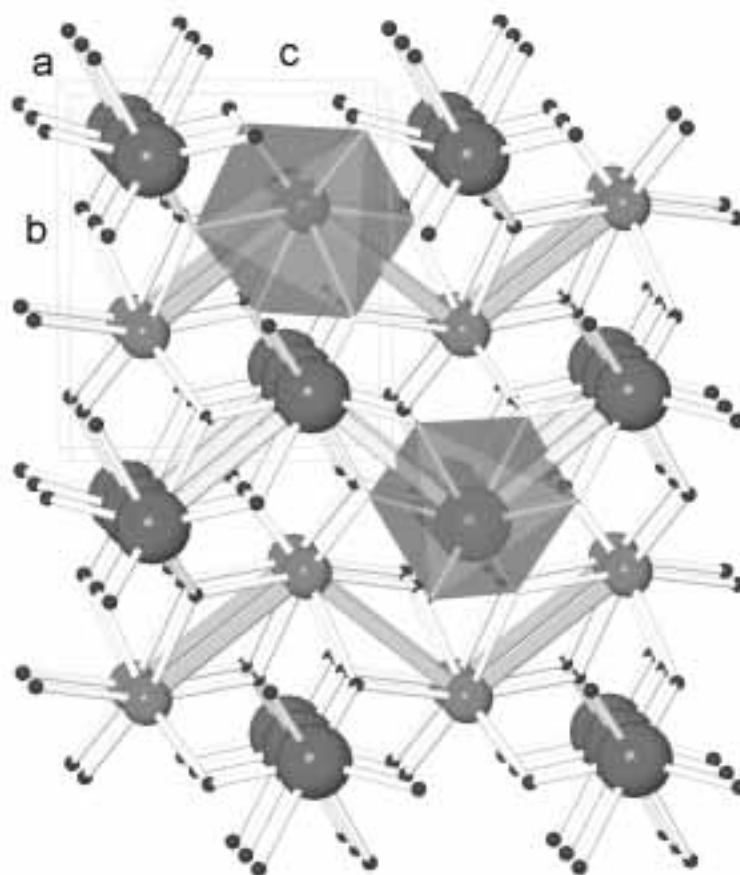


Figure 6 (a). D. Errandonea et al.

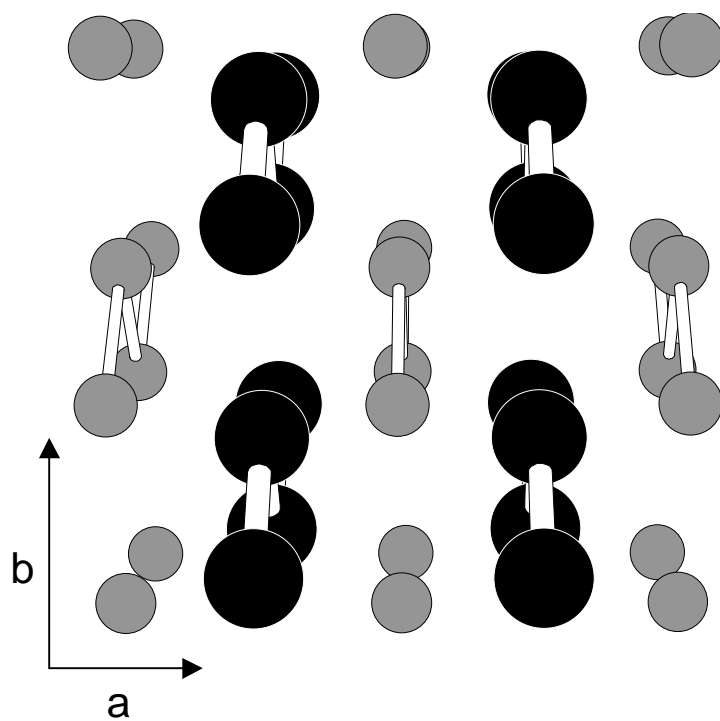


Figure 6 (b). D. Errandonea et al.

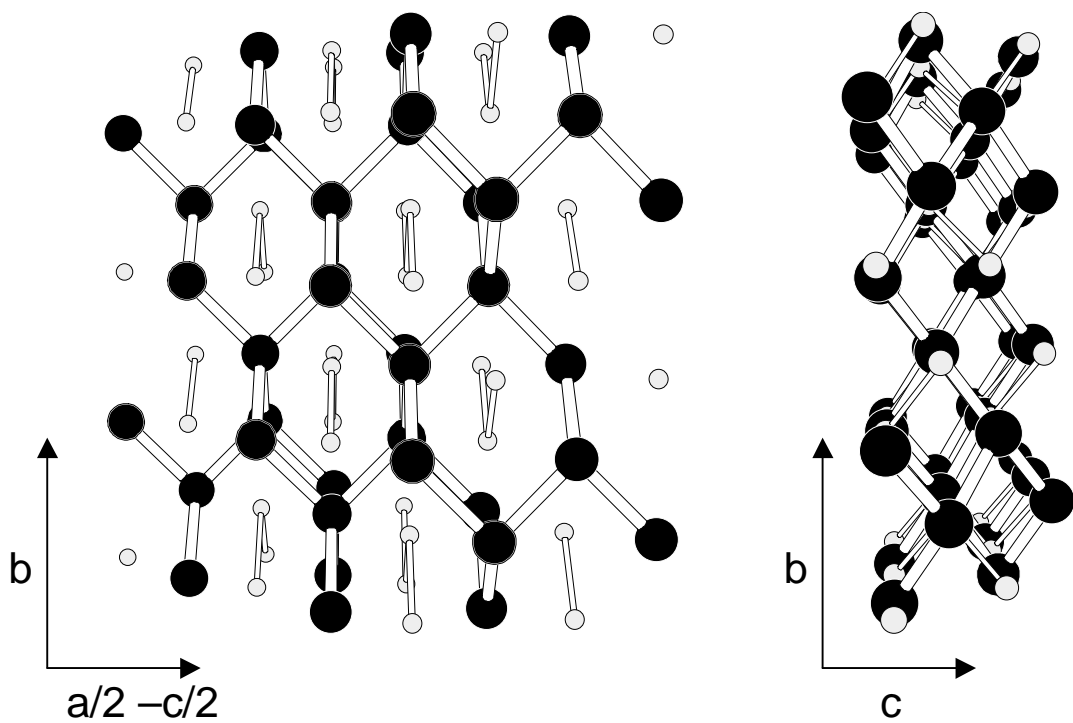


Figure 7. D. Errandonea et al.

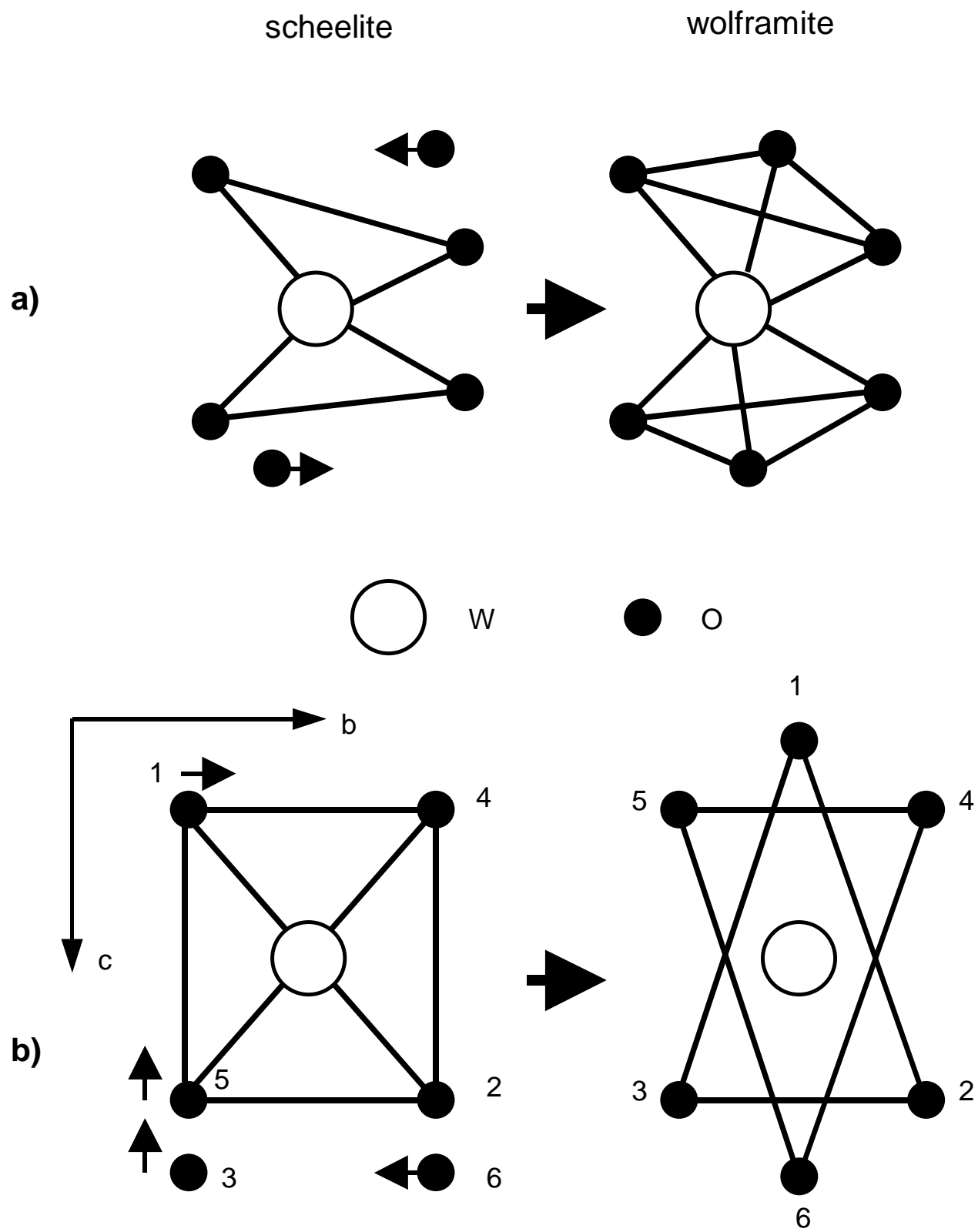


Figure 8. D. Errandonea et al.

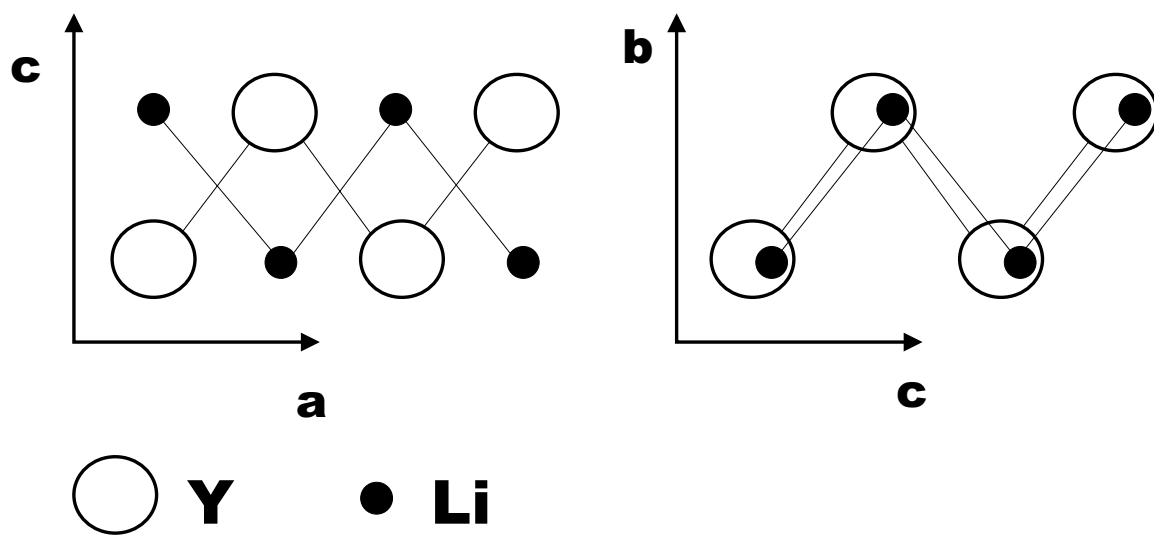


Figure 9. D. Errandonea et al.

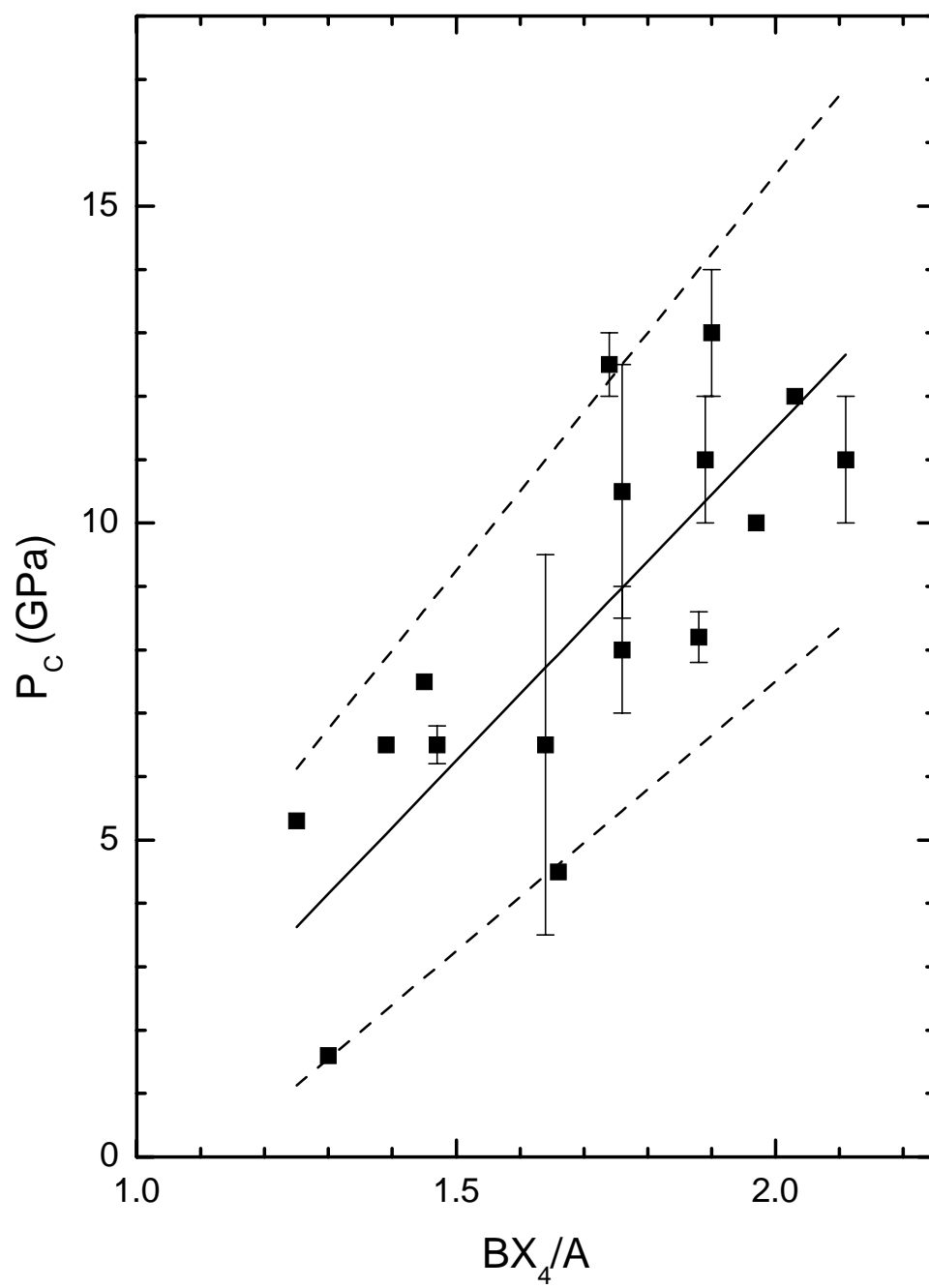


Figure 10. D. Errandonea et al.